Investigations of Nonstandard, Mickens-type, Finite-difference Schemes for Singular Boundary Value Problems in Cylindrical or Spherical Coordinates

Ron Buckmire
Mathematics Department, Occidental College, 1600 Campus Road, Los Angeles, California 90041-3338

Received 5 September 2002; accepted 4 October 2002

DOI 10.1002/num.10055

It is well known that standard finite-difference schemes for singular boundary value problems involving the Laplacian have difficulty capturing the singular ($\mathcal{O}(1/r)$ or $\mathcal{O}(\log r)$) behavior of the solution near the origin ($r = 0$). New nonstandard finite-difference schemes that can capture this behavior exactly for certain singular boundary value problems encountered in theoretical aerodynamics are presented here. These schemes are special cases of nonstandard finite differences which have been extensively researched by Professor Ronald E. Mickens of Clark Atlanta University in their most general form. Several examples of these "Mickens-type" finite differences that illustrate both their accuracy and utility for singular boundary value problems in both cylindrical and spherical co-ordinates are investigated. The numerical results generated by the Mickens-type schemes are compared favorably with solutions obtained from standard finite-difference schemes. © 2003 Wiley Periodicals, Inc. Numer Methods Partial Differential Eq 19: 380–398, 2003

Keywords: finite-difference schemes; theoretical aerodynamics; cylindrical or spherical coordinates

1. INTRODUCTION

This article introduces finite-difference schemes for computing numerical solutions to singular boundary value problems in spherical or cylindrical coordinates. These boundary value problems involve partial differential equations or ordinary differential equations that occur in theoretical aerodynamics and other fields. The schemes involve novel ways to discretize the Laplacian operator $\mathcal{R}_p \equiv r^p(d/dr)$, where $p = 1$ is the cylindrical case and $p = 2$ is the spherical

Correspondence to: Ron Buckmire (e-mail: buckmire@oxy.edu)
Contract grant sponsor: Occidental College Mathematics Department

case. These nonstandard finite-difference schemes are special cases of the numerical methods Professor Ronald E. Mickens of Clark Atlanta University has analyzed extensively for years ([1–3], etc.).

The scheme for the cylindrical case was initially presented in Buckmire's 1994 thesis [4] in which particular slender bodies of revolution were found to possess shock-free flows as specific numerical solutions of a mixed-type, singular boundary value problem. The problem is formulated using transonic small disturbance theory found in [5–7], among other sources. Cole and Schwendeman announced the first computation of a fore-aft, symmetric, shock-free transonic slender body in [8]. This work was expanded in [4], which led to the first computation of shock-free, transonic, slender bodies with axisymmetry but without fore-aft symmetry. Basically, the problem involves numerically solving a boundary value problem with an elliptic-hyperbolic partial differential equation (the Kármán-Guderley equation) in cylindrical coordinates, with a singular inner Neumann boundary condition at $r = 0$ and a non-singular outer Dirichlet boundary condition far away from $r = 0$. Namely,

$$(K - (\gamma + 1)\phi_x)\phi_{xx} + \phi_{\tilde{r}\tilde{r}} + \frac{1}{\tilde{r}}\,\phi_{\tilde{r}} = 0. \tag{1}$$

$$\begin{aligned} &\phi(x, \tilde{r}) \;\to\; S(x)\log \tilde{r} + G(x), && \text{as } \tilde{r} \to 0,\ |x| \le 1 \\ &\phi(x, \tilde{r}) \text{ bounded}, && \text{for } \tilde{r} = 0,\ |x| > 1. \end{aligned} \tag{2}$$

$$\phi(x, \tilde{r}) \;\to\; \frac{\mathcal{D}}{4\pi}\,\frac{x}{(x^2 + K\tilde{r}^2)^{3/2}}, \qquad \text{as } (x^2 + \tilde{r}^2)^{1/2} \to \infty. \tag{3}$$

In (1), (2), and (3) the variable $\tilde{r}$ is a scaled cylindrical coordinate, K is the transonic similarity parameter, $\mathcal{D}$ is a dipole strength, and $\phi(x, \tilde{r})$ is a velocity disturbance potential. Both $S(x)$ and $G(x)$ are bounded functions. The main point of sketching the boundary value problem here is to emphasize that the function $G(x)$, which occurs in (2) needs to be computed very accurately, because the pressure coefficient on the body depends directly on $G'(x)$. It is the pressure coefficient that allows the determination of whether the body possesses a shock-free flow. Computing it is complicated by the fact that $\phi(x, \tilde{r})$ and $S(x)\log \tilde{r}$ are becoming singular as $\tilde{r} \to 0$, which is where the boundary condition must be evaluated, and the quantity $G(x)$ we require is the difference between these two large quantities. Thus, a numerical method was needed to compute the solution $\phi(x, \tilde{r})$ particularly accurately as $\tilde{r} \to 0$. It was discovered that an exact, nonstandard finite-difference scheme existed for a simpler, related boundary value problem. This discovery was the motivation for adoption of the scheme introduced in [4] and analyzed and discussed in more detail in [9]. Upon further analysis the author found other nonstandard finite difference schemes that could be derived for slightly different boundary value problems, and then extended this concept to spherical coordinates. It is these results that are presented within.

The rest of this article shall continue by reproducing some illustrative examples of nonstandard finite differences presented by Mickens in [10]. In this section it shall be made clear that these "Mickens-type," nonstandard finite differences are robust numerical techniques that have surprisingly useful properties.

In the third section, the details of the derivation of the specific Mickens-type, finite-difference scheme introduced in [4] and detailed in [9] shall be discussed. In addition, the nonstandard scheme for the corresponding problem in spherical coordinates is also derived here. This involves looking at the discretization of the $\mathcal{R}_p$ operator for $p = 1$ (cylindrical coordinates) and $p = 2$ (spherical coordinates).

In the fourth section, the derivation of selected model boundary value problems is given, along with their exact solutions. In cylindrical coordinates this involves Bessel's functions and, in spherical coordinates, hyperbolic trigonometric functions. These model problems are related to the boundary value problem for $\phi(x, \tilde{r})$ described in (1), (2), and (3) but are chosen because they have known exact solutions which can be used as benchmarks for the numerical results. The details of how the finite-difference schemes can be used to produce approximations to these solutions are presented.

In the fifth section, the new Mickens-type schemes are applied to produce numerical solutions of these selected singular boundary value problems. Graphs of the error between the exact solution and the approximate solution generated from the standard scheme and the nonstandard scheme are given which illustrate the superior accuracy of the Mickens-type schemes.

The article ends with a conclusion and an appendix which details how the truncation error between the standard finite-difference approximation varies from that of the Mickens-type schemes.

2. NONSTANDARD FINITE DIFFERENCES

This section will recount the idea behind nonstandard finite differences, drawing heavily upon the work of Professor Ronald E. Mickens ([1–3, 10, 11]). Nonstandard finite differences are numerical methods which approximate derivatives and differential equations by using non-traditional discrete formulations. The general form of the traditional derivative can be expressed as

$$\frac{du}{dt} = \lim_{h \to 0} \frac{u(t + \psi_1(h)) - u(t)}{\psi_2(h)} = \lim_{h \to 0} \frac{u(t + h) - u(t)}{h} \tag{4}$$

with

$$\psi_n(h) = h + \mathcal{O}(h^2). \tag{5}$$

This leads to a generalized form of the discretization of the derivative

$$\frac{du}{dt} \approx \frac{u_{k+1} - u_k}{\phi(h, \lambda)}. \tag{6}$$

It is usually the nonlinear form of the "denominator function" $\phi(h, \lambda)$ which determines that this discretization will be part of a nonstandard finite difference scheme. In [3] some examples of denominator functions which have the desired qualities listed in (5) are provided and reproduced

below in (7). Obviously, the first denominator function would result in the traditional derivative found in (4).

$$\phi(h) = \begin{cases} h, \\ \sin(h), \\ e^h - 1, \\ 1 - e^{-h}, \\ \dfrac{1 - e^{-\lambda h}}{\lambda}, \\ \vdots \end{cases} \tag{7}$$

In the limit, using any of the above sample denominator function results in the familiar forward definition of the derivative seen in (4). However, for finite h, which is, of course the typical computational practice, the denominator function will produce a discrete derivative that is close to the typical derivative but one which can deviate interestingly from it, depending on the size of h.

One of the most important results Mickens proves in [2] is that *every* ordinary differential equation (ODE) can be represented by an *exact* finite-difference scheme (OΔE). In other words, if the exact solution of the ODE is denoted by $u(t)$ and the discrete representations of the solution are denoted by u_k, then there exists a numerical scheme for which $u(t_k) = u_k$ for all $t_k = kh$ comprising the discrete domain on which the solution is being computed, for all grid separations h.

Consider the standard ODE:

$$\frac{dy}{dt} = -\lambda t,$$

which has the exact solution $y(t) = y_0 e^{(t-t_0)}$. The standard finite-difference scheme would be to use a forward Euler method so that the OΔE would be

$$\frac{y_{k+1} - y_k}{h} = -\lambda y_k.$$

However, Mickens points out ([3], p. 74) that the following nonstandard finite-difference scheme

$$\frac{y_{k+1} - y_k}{\left(\dfrac{1 - e^{-h\lambda}}{\lambda}\right)} = -\lambda y_k$$

is exact. The above OΔE can be solved to produce a discrete version of the exact solution, $y_{k+1} = y_k e^{-\lambda h}$.

He also provides less obvious examples of exact finite-difference schemes for some basic ordinary differential equations. For example, the initial value problem

$$\frac{dy}{dt} = y^2, \qquad y(t_0) = y_0 \tag{8}$$

has the exact solution $y(t) = y_0/([1 - y_0(t - t_0)]$. The standard finite-difference scheme would be

$$\frac{y_{k+1} - y_k}{h} = y_k^2, \tag{9}$$

which has the inaccurate solution $y_{k+1} = y_k(1 + hy_k)$. However, Mickens points out that the previous finite-difference scheme can be made to be exact for (8) by choosing a "nonlocal" discretization of the ODE. This new nonstandard scheme looks like

$$\frac{y_{k+1} - y_k}{h} = y_k y_{k+1}. \tag{10}$$

It is easy to see that the above can be rearranged to produce $y_{k+1} = y_k/(1 - hy_k)$, which is simultaneously the solution to the OΔE in (10) and the discrete form of the solution to the ODE in (8).

Note that we have presented two different ways that a standard finite-difference scheme can be modified to make it nonstandard. In the examples presented here the error of the nonstandard scheme was *zero.* The discovery of a similar exact nonstandard discretization of the radial derivatives of the Laplacian in cylindrical coordinates led to the scheme used in [4] and is discussed in section 3 of this article. In honor of Professor Mickens' extensive work on these nonstandard finite-difference schemes the author proposes that they be referred to as "Mickens-type" finite-difference schemes, or simply "Mickens differences."

3. DISCRETIZING THE OPERATOR $\mathcal{R}_p \equiv r^p(d/dr)$

This section shall explain the discretization of the Laplacian operator $\mathcal{R}_p = r^p(d/dr)$, where $p = 1$ or $p = 2$. Laplace's equation in cylindrical coordinates is given by

$$\frac{1}{r}(ru_r)_r + u_{\theta\theta} = 0$$

and clearly contains the $\mathcal{R}_1$ operator. Laplace's equation in spherical coordinates is given by

$$\frac{1}{r^2}(ru_r)_r + u_{\theta\theta} = 0$$

and clearly contains the $\mathcal{R}_2$ operator. The Kármán-Guderley equation (1) which was the subject of [4] also contains $\mathcal{R}_1$, the radial derivatives of the Laplacian in cylindrical coordinates. Consider $B(r)$ which is defined as

$$B(r) = \mathcal{R}_p u = \frac{r^p du}{dr},$$

where $u = u(r)$ is an unknown function (the solution) the operator $\mathcal{R}_p$ acts on. The problem at hand requires determining a numerical discretization or approximation for $\mathcal{R}_p$.

The first step in the discretization of the operator is to choose a grid $\{r_j\}_{j=0}^N$ on the interval $0 \le r \le 1$ where

$$0 \leftarrow r_0 < r_1 < r_2 < \cdots < r_j < \cdots < r_N = 1. \tag{11}$$

3.1. The Cylindrical Case

For the cylindrical case, let $p = 1$ and the operator becomes $\mathcal{R}_1 = r(d/dr)$. On the grid defined in (11) one has discrete forms of the quantities of interest, such as $u(r_j) = u_j$ and

$$B_{j+1/2} = r \left.\frac{d}{dr}\right|_{r=r_{j+1/2}} \qquad \text{where } r_{j+1/2} = \frac{r_j + r_{j+1}}{2},$$

i.e., in between grid points.

There are several choices for discretizing $B(r)$, but the standard forward-difference approximation method and the new nonstandard scheme were selected and will be compared with each other. Note that the discrete quantity B is actually defined in between grid points, not on them.

$$B^{(1)}_{j+1/2} = r_{j+1/2} \frac{u_{j+1} - u_j}{r_{j+1} - r_j} \tag{12}$$

$$B^{(2)}_{j+1/2} = \frac{u_{j+1} - u_j}{\log(r_{j+1}) - \log(r_j)} = \frac{u_{j+1} - u_j}{\log(r_{j+1}/r_j)} \tag{13}$$

The standard scheme in (12) shall be referred to as Scheme (1) and the new scheme in (13) shall be referred to as Scheme (2). Scheme (2) can be obtained by assuming that $B(r)$ should be constant on each subinterval $[r_j, r_{j+1}]$ of the grid. If one relates $B(r)$ back to the physical fluid mechanics problem we want to solve, it corresponds to a mass flux. The relationship between $B_{j+1/2}$ and u_j and u_{j+1} solves the simple boundary value problem

$$ru' = B_{j+1/2} = \text{constant} \tag{14}$$

$$u(r_j) = u_j \tag{15}$$

$$u(r_{j+1}) = u_{j+1}. \tag{16}$$

The solution to this is $u(r) = B_{j+1/2} \log r + C$, which, when one applies the boundary conditions (15) and (16) leads to the formula

$$B_{j+1/2} = \frac{u_{j+1} - u_j}{\log(r_{j+1}/r_j)}.$$

Thus, Scheme (2) is a Mickens-type, nonstandard, exact finite-difference scheme for the ODE

$$r\frac{du}{dr} = B, \qquad \text{where } B \text{ is a known constant.} \tag{17}$$

3.2. The Spherical Case

In a similar fashion to the procedure outlined above, a nonstandard, exact finite-difference scheme can be obtained for the spherical analogue to (17). The spherical version of the ODE comes from setting $\mathcal{R}_2 u$ equal to a constant, producing

$$r^2\frac{du}{dr} = A, \qquad \text{where } A \text{ is a known constant.} \tag{18}$$

Even though it does not have the same physical significance of a mass flux as it did in cylindrical co-ordinates, we can still obtain a relationship between $A_{j+1/2}$, u_j, and u_{j+1} by solving (18) using the conditions (15) and (16). The solution in this case is $u(r) = -A/r + C$, which when one applies the boundary condition leads to the OΔE

$$A_{j+1/2} = \frac{u_{j+1} - u_j}{\left(-\dfrac{1}{r_{j+1}}\right) - \left(-\dfrac{1}{r_j}\right)}.$$

This can be rearranged to produce

$$A^{(2)}_{j+1/2} = r_j r_{j+1}\frac{u_{j+1} - u_j}{r_{j+1} - r_j}. \tag{19}$$

This formula is a Mickens-type, exact, nonstandard finite-difference scheme for (18). The standard finite-difference scheme for this ODE would be

$$A^{(1)}_{j+1/2} = r^2_{j+1/2}\frac{u_{j+1} - u_j}{r_{j+1} - r_j}. \tag{20}$$

Notice that in the spherical Mickens-type scheme (19) it is the nonlocal discretization of r^2, which makes it nonstandard. In the cylindrical Mickens-type scheme (13) it is the presence of nonlinear functions (logarithms) and the nonlocal discretization, which make it nonstandard. Regardless, both schemes have zero local truncation error; they are exact. The superscripts in (19) and (20) are used to indicate the difference between the nonstandard and standard discretizations in spherical coordinates in a similar way the OΔEs (13) and (12) in cylindrical coordinates were differentiated from each other.

3.3. Informal Derivation of the Nonstandard Schemes

One can also derive the form of the nonstandard schemes by using a more intuitive but less rigorous approach involving differentials. The ODE is rearranged through the use of differentials, and then the differentials are approximated by finite Δs.

$$B = r\frac{du}{dr} = \frac{du}{\frac{dr}{r}} = \frac{du}{d(\log(r))} \approx \frac{\Delta u}{\Delta(\log(r))}.$$

This approximate version of the rearranged ODE is actually Scheme (2) (13).

$$\frac{\Delta u}{\Delta(\log(r))} = \frac{u_{j+1} - u_j}{\log(r_{j+1}) - \log(r_j)} = B^{(2)}_{j+1/2}.$$

Similarly, one can derive the spherical version of Scheme (2) found in (19) by rearranging the ODE in (18):

$$A = r^2\frac{du}{dr} = \frac{du}{\frac{dr}{r^2}} = \frac{du}{d\left(-\frac{1}{r}\right)} \approx \frac{\Delta u}{\Delta\left(-\frac{1}{r}\right)} = \frac{u_{j+1} - u_j}{\left(-\frac{1}{r_{j+1}}\right) - \left(-\frac{1}{r_j}\right)} = r_j r_{j+1}\frac{u_{j+1} - u_j}{r_{j+1} - r_j} = A^{(2)}_{j+1/2}.$$

In this section the derivation of Mickens-type, finite-difference schemes that discretize the $\mathcal{R}_p$ operator in cylindrical or spherical coordinates were given. The new schemes were presented adjacent to the standard finite-difference methods for the same Laplacian operator to highlight the unusual features of the nonstandard schemes. In the next section, both types of schemes will be applied to particular singular boundary value problems to demonstrate the superior utility of the Mickens-type schemes.

4. APPLYING THE SCHEMES

To illustrate the efficacy and accuracy of the Mickens-type schemes derived in (13) and (19), they will be applied to a number of singular boundary value problems related to the original problem solved in [4]. This section will present the solution of these boundary value problems as well as the details of how the finite-difference schemes can be used to generate numerical approximations to them.

The Kármán-Guderley equation (1) and the associated boundary conditions of (2) and (3) can be directly related to the simple boundary value problem given below

$$\frac{1}{r}\frac{d}{dr}\left(r\frac{du}{dr}\right) - m^2 u = 0, \qquad m \text{ constant} \tag{21}$$

$$r\frac{du}{dr}\bigg|_{r=0} = S, \tag{22}$$

$$u(1) = G. \tag{23}$$

If one linearizes and substitutes $\phi(x, r) = u(r)e^{imx}$ into (1), one will obtain the above singular boundary value problem. This simple boundary value problem is used as the "model problem" to benchmark the new finite-difference scheme instead of the problem containing the transonic

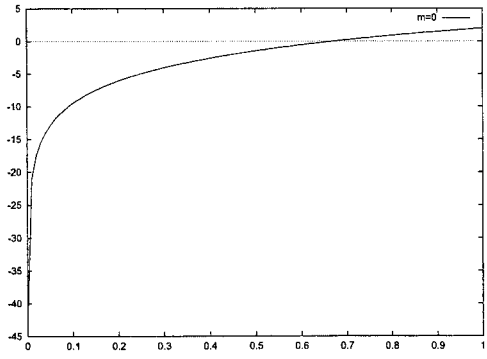

(a) The $m = 0$ cylindrical solution in (24)

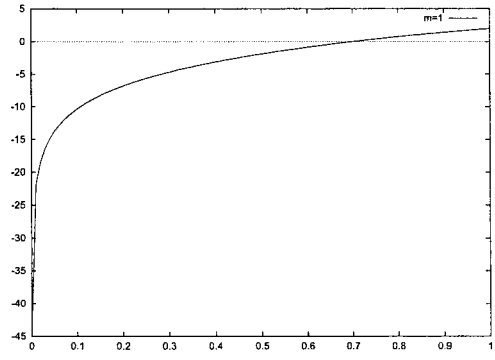

(b) The $m = 1$ cylindrical solution in (25)

FIG. 1. Exact solutions for the cylindrical model problem.

small-disturbance equation (1) one is really interested in solving. The reason is that the simpler problem has a known exact solution involving logarithms or Bessel functions, depending on the value of m, where m is a natural number. The model problem retains the essential singular nature of the aerodynamics problem. The exact solutions to the model boundary value problem in cylindrical coordinates can be written as

$$m = 0, \quad u(r) = S \log r + G \tag{24}$$

$$m > 0, \quad u(r) = \frac{-\pi}{2} S K_0(rm) + \left(G + S \frac{\pi}{2} K_0(m) \frac{I_0(rm)}{I_0(m)} \right). \tag{25}$$

Note that solutions to the cylindrical model problem have the required singular behavior ($\log r$)) as $r \to 0$, as can be seen in Fig. 1.

4.1. The $m = 0$ Cylindrical Case

First consider the $m = 0$ model problem. The differential equation in this case is simply

$$\frac{1}{r} \frac{d}{dr} \left(r \frac{du}{dr} \right) = B'(r) = 0.$$

This has the simple solution $B(r) =$ constant. Using the boundary condition at $r = 0$, $B(0) = S \Rightarrow B(r) = S$. Thus, the discrete version of the model equation that is being solved is

$$B_{j+1/2} = S. \tag{26}$$

Using Scheme (1) (the standard forward-difference approximation),

$$B_{j+1/2} = r_{j+1/2} \frac{u_{j+1} - u_j}{r_{j+1} - r_j} = S \Rightarrow u_j = u_{j+1} - 2S \frac{r_{j+1} - r_j}{r_{j+1} + r_j}, \qquad \text{with } u_N = G. \tag{27}$$

This is a simple marching scheme which allows one to compute all the u_j, $j = 0, \ldots, N$ starting from $u_N = G$ and "marching" down to u_0.

Using Scheme (2) (the nonstandard scheme), the discrete equation to be solved is

$$B_{j+1/2} = \frac{u_{j+1} - u_j}{\log(r_{j+1}/r_j)} = S \Rightarrow u_j = u_{j+1} - S \log\left(\frac{r_{j+1}}{r_j}\right), \qquad \text{with } u_N = G. \tag{28}$$

Scheme (2) also leads to a marching scheme that solves the model equation exactly *by definition.* This happens because the scheme was derived assuming that $B(r)$ would be constant on each subinterval. For this model equation $B(r) = S$, so it is the same constant, namely S on each subinterval. So Scheme (2) is exact for this model equation where $m = 0$. Scheme (1) has a significant numerical error that gets worse as the computed solution approaches the singularity at the origin. These results are displayed graphically in the figures in Section 5.

4.2. The $m \neq 0$ Cylindrical Case

When $m \neq 0$ the model differential equation in (21) becomes

$$r^2u'' + ru' - m^2r^2u = 0, \tag{29}$$

which after the scaling $s = mr$ can be seen to be the zeroth-order Bessel's equation

$$s^2u'' + su' - s^2u = 0.$$

Using a standard discretization, the OΔE for the $m \neq 0$ form of (21) is

$$\frac{1}{r_j}\left(r_{j+1/2}\frac{u_{j+1} - u_j}{r_{j+1} - r_j} - r_{j-1/2}\frac{u_j - u_{j-1}}{r_j - r_{j-1}}\right) - m^2u_j = 0. \tag{30}$$

The nonstandard discretization will be

$$\frac{1}{r_j}\left(\frac{u_{j+1} - u_j}{\log(r_{j+1}/r_j)} - \frac{u_j - u_{j-1}}{\log(r_j/r_{j-1})}\right) - m^2u_j = 0. \tag{31}$$

In the $m \neq 0$ cases one can not simply produce a marching scheme as in the $m = 0$ cases [(27) and (28)], so the solutions are obtained by solving a tri-diagonal system of equations for $\{u_j\}_{j=0}^N$. Of course, exact solutions can be found for both the $m = 0$ and $m \neq 0$ cases. In the $m \neq 0$ case the nonstandard scheme is not exact, but it can be clearly seen from the numerical results given in Section 5 that it does a better job of approximating the exact solution than the standard scheme does, especially near the $r = 0$ singularity.

4.3. Model Problem in Spherical Coordinates

The model problem in spherical coordinates is not directly motivated from the Kármán-Guderley boundary value problem as the cylindrical version is. It is simply an analogous extrapolation from the cylindrical model problem given in (21),

$$\frac{1}{r^2}\frac{d}{dr}\left(r^2\frac{du}{dr}\right) - n^2u = 0, \qquad n \text{ constant} \tag{32}$$

$$r^2\frac{du}{dr}\bigg|_{r=0} = S, \tag{33}$$

$$u(1) = G. \tag{34}$$

However, in spherical coordinates the inner Neumann boundary condition (33) is not physically significant so there are other choices which can be made for this inner boundary condition, such as a simple Dirichlet condition. This choice would make the exact solution to the model problem given above even simpler. The exact solution of the model spherical ODE can be found to consist of hyperbolic sines and cosines after noticing that (32) can be rewritten (when $n \neq 0$) as

$$r^2u'' + 2ru' - n^2r^2u = 0. \tag{35}$$

This looks very similar to the Bessel's equation from the cylindrical coordinates problem (29), but the solutions are very different. The derivatives can be grouped so that if $v = ru$ the equation becomes

$$\begin{aligned} r^2u'' + 2ru' - n^2r^2u &= (ru)'' - n^2(ru) \\ &= v'' - n^2v \\ &= 0 \end{aligned}$$

The general solution to (35) is

$$u(r) = C_1\frac{\sinh(nr)}{r} + C_2\frac{\cosh(nr)}{r}.$$

The exact solutions to the model boundary value problem in spherical coordinates given in (32), (33) and (34) can be written as

$$n = 0, \qquad u(r) = -\frac{S}{r} + S + G \tag{36}$$

$$n > 0, \qquad u(r) = \frac{-S\cosh(nr)\sinh(n) + (G + S\cosh(n))\sinh(nr)}{r\sinh(n)}. \tag{37}$$

These solutions above also exhibit singular behavior as $r \to 0$, albeit much more strongly than their cylindrical coordinate counterparts. The solutions in spherical coordinates have singular behavior ($\mathcal{O}(1/r)$) as $r \to 0$. This can be seen graphically in Fig. 2.

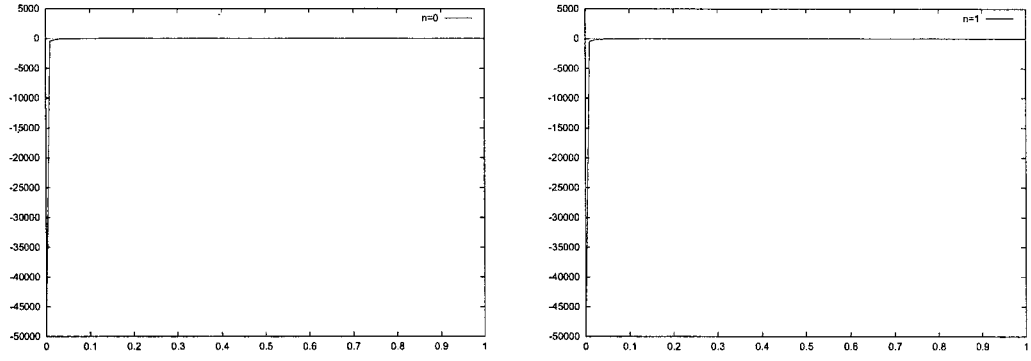

(a) The $n = 0$ spherical solution in (36) (b) The $n = 1$ spherical solution in (37)

FIG. 2. Exact solutions for the spherical model problem.

4.4. $n = 0$ Spherical Case

First consider the $n = 0$ model problem. The differential equation in this case is simply

$$\frac{1}{r^2}\frac{d}{dr}\left(r^2\frac{du}{dr}\right) = \frac{1}{r^2}A'(r) = 0.$$

This has the simple solution $A(r) =$ constant. Rewriting the Neumann boundary condition (33) at $r = 0$ as $A(0) = S$ implies $A(r) = S$.

The discrete version of the model equation which is being solved is

$$A_{j+1/2} = S. \tag{38}$$

Using the standard forward-difference approximation produces

$$A^{(1)}_{j+1/2} = r^2_{j+1/2}\frac{u_{j+1} - u_j}{r_{j+1} - r_j} = S \Rightarrow u_j = u_{j+1} - S\frac{r_{j+1} - r_j}{r^2_{j+1/2}} \qquad \text{with } u_N = G. \tag{39}$$

Now we have a simple marching scheme similar to the one utilized in (27), which allows one to compute all the u_j, $j = 0, \ldots, N$ starting from $u_N = G$ and marching down to u_0.

Using the Mickens-type scheme the discrete equation to be solved is

$$A^{(2)}_{j+1/2} = r_j r_{j+1}\frac{u_{j+1} - u_j}{r_{j+1} - r_j} = S \Rightarrow u_j = u_{j+1} - S\frac{r_{j+1} - r_j}{r_{j+1}r_j} \qquad \text{with } u_N = G. \tag{40}$$

The nonstandard Scheme (2) leads to a marching scheme which again solves the model equation exactly *by definition.* This happens because this scheme was derived assuming that $A(r)$ would be constant on each subinterval. For the model equation $A(r) = S$, so A equals the same constant, namely S on each subinterval. Thus Scheme (2) is exact for the model equation (35) where $n = 0$. The standard Scheme (1), on the other hand, has a significant numerical error that gets worse as its computed solution approaches the singularity at the origin.

4.5. The $n \neq 0$ Spherical Case

Using a standard discretization the OΔE for the $n \neq 0$ form of (32) is

$$\frac{1}{r_j^2}\left(r_{j+1/2}^2 \frac{u_{j+1}-u_j}{r_{j+1}-r_j} - r_{j-1/2}^2 \frac{u_j-u_{j-1}}{r_j-r_{j-1}}\right) - n^2 u_j = 0. \tag{41}$$

The nonstandard discretization will be

$$\frac{1}{r_j^2}\left(r_j r_{j+1} \frac{u_{j+1}-u_j}{r_{j+1}-r_j} - r_j r_{j-1} \frac{u_j-u_{j-1}}{r_j-r_{j-1}}\right) - n^2 u_j = 0. \tag{42}$$

Like the $m \neq 0$ cylindrical case, the $n \neq 0$ spherical case does not produce a marching scheme as in the $m = 0$ and $n = 0$ cases, so the solutions are obtained by solving a tri-diagonal system of equations for $\{u_j\}_{j=0}^N$. Fortunately, exact solutions can be found for all values of m (cylindrical cases) and n (spherical cases). In the $n \neq 0$ cases the Mickens-type scheme (42) is not exact, but the numerical results given in section 5 will demonstrate that it does a much better job of approximating the exact solution than the standard scheme (42) does.

5. NUMERICAL RESULTS

In this section the numerical results will be given which indicate the effectiveness of the Mickens-type schemes in approximating the operator $\mathcal{R}_p = r^p(du/dr)$. This is done by comparing the solutions to the cylindrical and spherical model problems generated by the numerical schemes given in (31) and (30) and in (42) and (41) to the exact solutions given in (24) and (25) and in (36) and (37).

Numerically one can not actually evaluate the Neumann boundary conditions (22) and (33) at $r = 0$ exactly. Instead one chooses a small parameter ϵ and evaluates the boundary condition at $r = \epsilon$ repeatedly with values of ϵ that approach zero. For the results displayed in Fig. 3, $\epsilon = 0.1$, 0.01, 0.001, 0.0001, and 0.00000001. It is these results which demonstrate the ability of the nonstandard scheme to handle the singular nature of the pertinent boundary value problems.

The new Mickens-type scheme in cylindrical coordinates (31) and spherical coordinates (42) are exact (zero error) in the $m = 0$ and $n = 0$ cases, respectively. Thus, in these cases we only need to compare the standard scheme to the new schemes, and we will obtain the exact error made by the standard scheme.

For the $m \neq 0$ and $n \neq 0$ cases we need to compare the nonstandard scheme's solution, the standard scheme's solution, and the exact solution to each other. In addition, because the motivation for the scheme was the ability to evaluate the solution near $r = 0$, the comparison of the numerical solutions with the exact solution at ever smaller values of ϵ is important. Figure 3 depicts the error between the exact solution and the numerical solution that each numerical method makes as the Neumann boundary conditions (22) and (33) are approximated at ever smaller values of r ($\epsilon \to 0$) for both the cylindrical and spherical model boundary value problems.

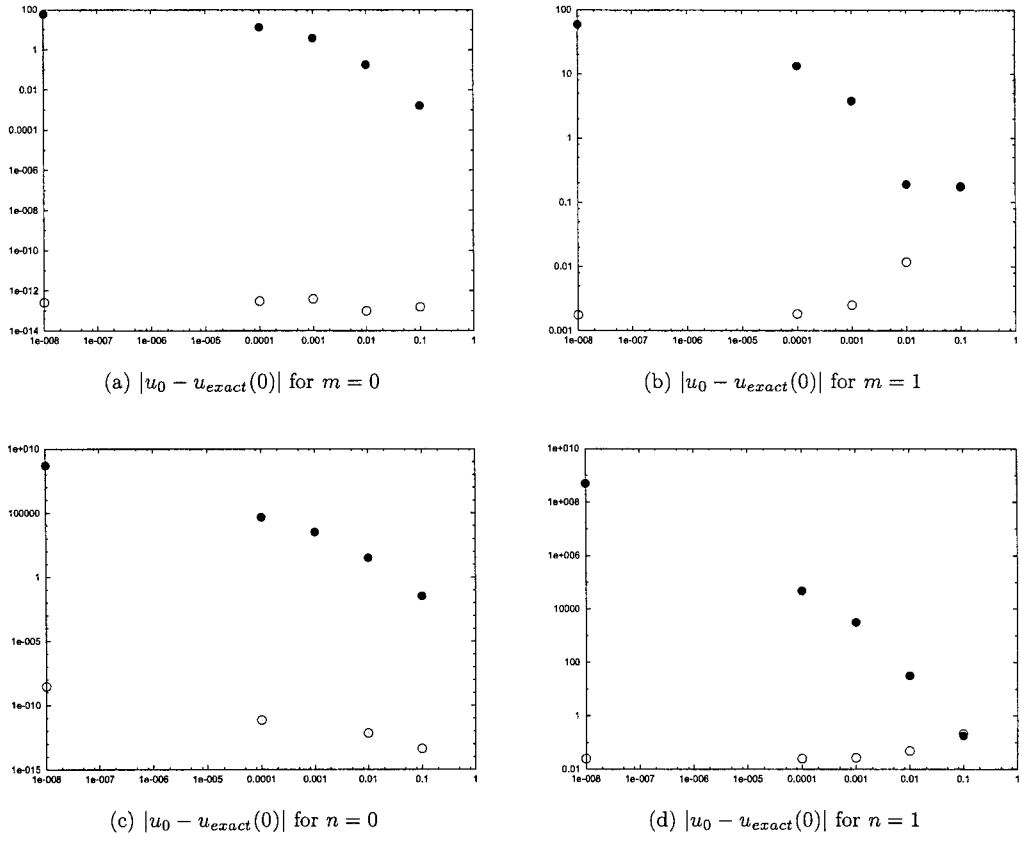

(a) $|u_0 - u_{exact}(0)|$ for $m = 0$

(b) $|u_0 - u_{exact}(0)|$ for $m = 1$

(c) $|u_0 - u_{exact}(0)|$ for $n = 0$

(d) $|u_0 - u_{exact}(0)|$ for $n = 1$

FIG. 3. Numerical error at $r = \epsilon \to 0$ for cylindrical ($m = 0$ and $m = 1$) and spherical ($n = 0$ and $n = 1$) data.

As one can see from the graphs of the exact solutions to the $m = 0$ and $m = 1$ problems, they are very similar. However, the two types of finite-difference schemes approximate the solutions to these problems with wildly varying accuracy, with the Mickens-type scheme being more successful by *orders of magnitude.* At $r = \epsilon = 0.0001$ the standard scheme produces an error of about 10^2, whereas the nonstandard scheme produces an error of about 10^{-1}. In Fig. 4 the graphs show the error on a log-log scale with each curve representing a solution computed at a different value of ϵ. Notice in Fig. 4(b) that the nonstandard scheme's error actually *decreases* as the boundary condition is evaluated at a more singular value closer to the origin, while the reverse is true for the standard scheme in Fig. 4(a).

The corresponding graphs of the error made by the two competing schemes in solving the spherical model problem are given below in Fig. 5. In Fig. 5(a) one can notice that the order of magnitude of the error made by the standard scheme is gigantic ($\approx 10^4$), whereas in Fig. 5(b) it is clear that the nonstandard scheme has only a modest error ($\approx 10^{-1}$), even when the inner boundary condition is being evaluated at the relatively small value of $\epsilon = 0.0001$.

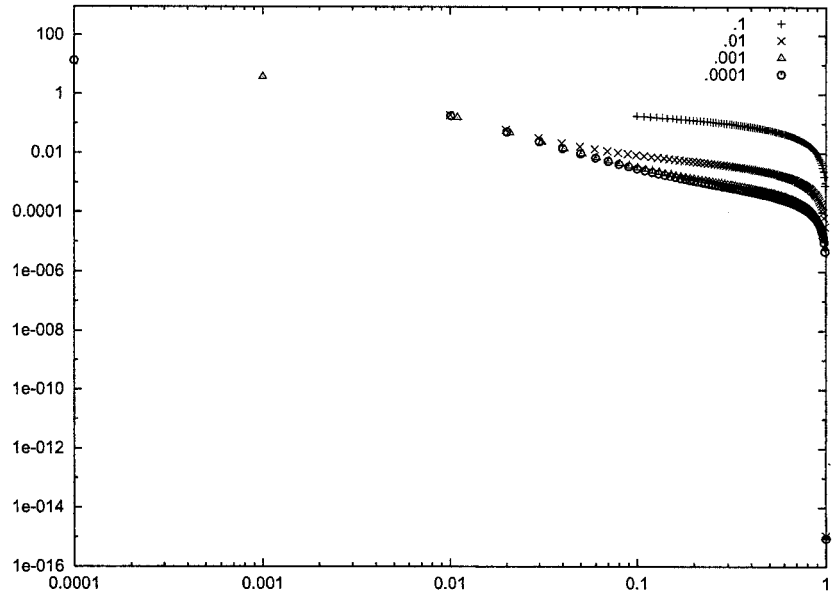

(a) $m = 1$ standard error

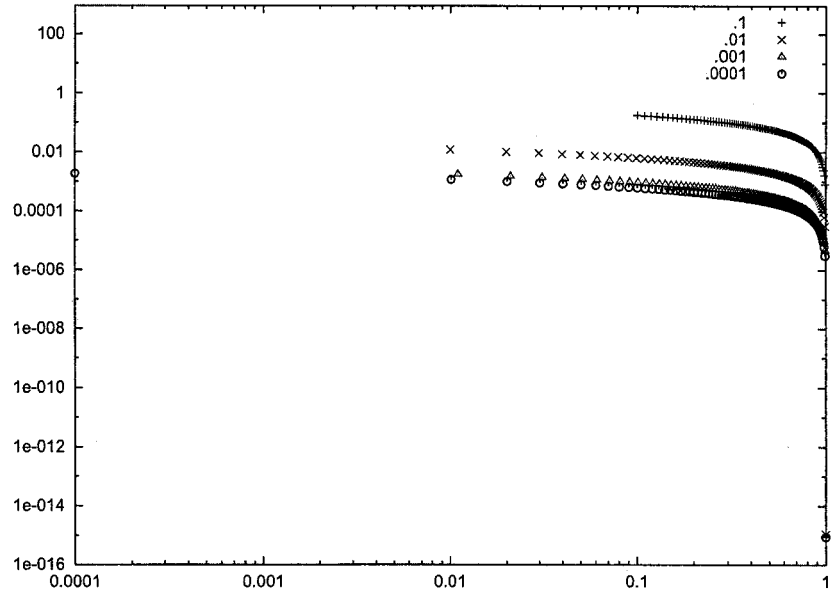

(b) $m = 1$ nonstandard error

FIG. 4. Numerical error comparison as $\epsilon \to 0$ for cylindrical solutions of (21).

All the calculations performed in this section used a uniform discrete grid with $N = 101$ grid points, with a grid separation which varied depending on ϵ. The known constants in the boundary conditions were taken to be $G = 2$ and $S = 5$ for no particular reason.

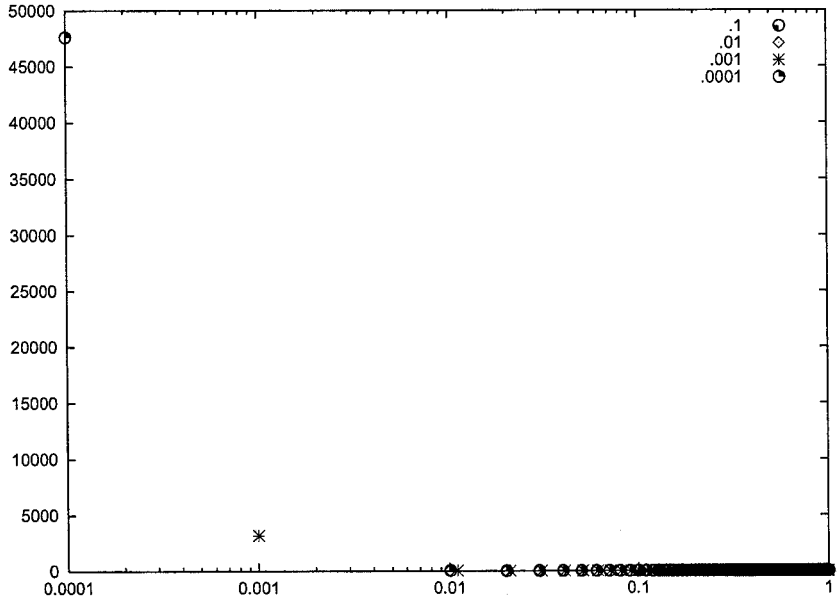

(a) $n = 1$ standard error

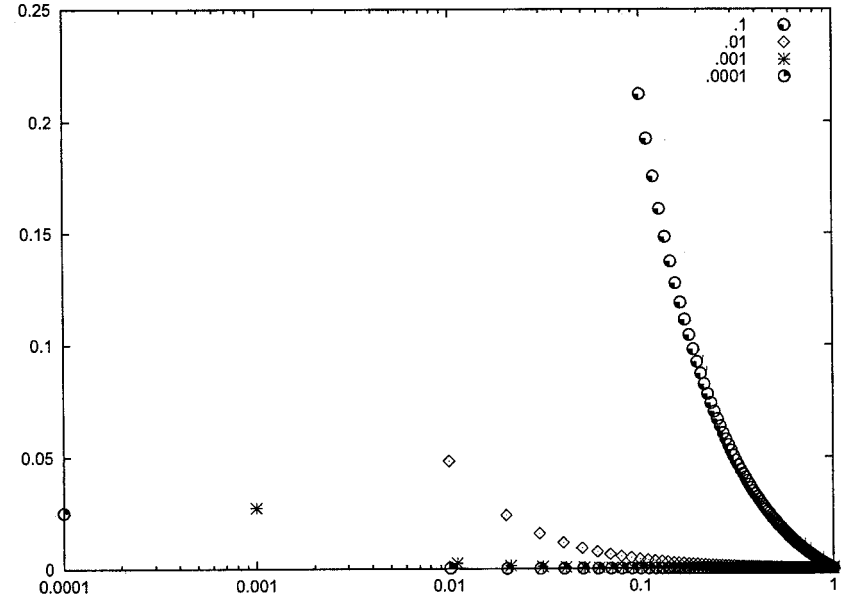

(b) $n = 1$ nonstandard error

FIG. 5. Numerical error comparison as $\epsilon \to 0$ for spherical solutions of (32).

A uniform grid is a bad choice to pick when discretizing the domain if one is solving a differential equation with a $r^p(d/dr)$ operator and the domain includes the singular point $r = 0$. In [9] it was shown that the error between the standard and nonstandard schemes depends on a

property of the grid defined as $\delta_j = (r_{j+1} - r_j)/(r_{j+1} + r_j)$. A better grid choice is to ensure that the grid has the property that δ_j is small for all j. The easiest way to do that is to pick one value of δ for all j. The value can be chosen by looking at the definition of δ_j and rearranging it to give a marching scheme that chooses the appropriate grid discretization $\{r_j\}_{j=0}^{N}$.

$$\delta_j = \frac{r_{j+1} - r_j}{r_{j+1} + r_j} \Rightarrow r_j = \left(\frac{1 - \delta_j}{1 + \delta_j}\right) r_{j+1}, \qquad \text{with } r_N = 1.$$

For example, if one lets $\delta_j = 1/N$, then

$$r_j = \left(\frac{1 - 1/N}{1 + 1/N}\right) r_{j+1} = \frac{N - 1}{N + 1}\, r_{j+1},$$

which implies that $r_j = \alpha^{N-j} r_N$, for $j = 0$ to N, where $\alpha = (N - 1)/(N + 1) < 1$. This grid choice corresponds to an approximately exponentially stretched grid, with many points clustered near $r = 0$. This analysis supports the selection of an exponentially scaled grid used by Krupp and Murman [12] and Cole and Murman [13] to numerically solve the Kármán-Guderley equation in the early 1970s.

The standard forward-difference scheme can be used to solve singular differential equations, but the grid must be chosen intelligently. Using the Mickens-type schemes there is flexibility about what kind of grid to use because they are still more accurate regardless of the grid choice.

6. CONCLUSIONS

In this article, new finite-difference schemes have been introduced to solve singular boundary value problems with differential equations in cylindrical or spherical coordinates. The given results show that these schemes appear to tackle singular boundary value problems more accurately and efficiently than standard finite-difference schemes. In particular, the nonstandard schemes easily approximate the solution near the singularity at the origin where the standard schemes generally fail. The numerical methods investigated here are interesting examples of the type of nonstandard finite-difference schemes that have been thoroughly researched by Professor Ronald E. Mickens. Although the initial discovery of these particular Mickens-type finite differences was motivated by a problem in theoretical aerodynamics in cylindrical coordinates, the schemes explicated within can really be used for any problem where the Laplacian operator in cylindrical or spherical coordinates needs to be discretized numerically. Future research will investigate applying the ideas in this article to other diverse boundary value problems in order to discover other useful Mickens-type, nonstandard finite-difference schemes.

APPENDIX: TRUNCATION ERRORS

Another way that one can compare two finite-difference schemes is to look at their local truncation errors. If one assumes the grid is uniform with grid separation parameter h, and let $r_j = jh$, $r_{j+1} = (j + 1)h = j + h$, $u_j = u(r_j)$ and $u_{j+1} = u(r_{j+1}) = u(r_j + h)$, then one can perform Taylor Expansions on the finite-difference schemes and obtain the truncation error associated with each approximation technique.

The standard finite-difference approximation of $(1/r)(ru')'$ looks like

$$\frac{1}{rh}\left(\left(r+\frac{h}{2}\right)\frac{u(r+h)-u(r)}{h}-\left(r-\frac{h}{2}\right)\frac{u(r)-u(r-h)}{h}\right)$$
$$=\frac{1}{r}(ru')'+\frac{h^2}{12}\left(u^{(iv)}+\frac{2u'''}{r}\right)+\frac{h^4}{360}\left(u^{(vi)}+\frac{3u^{(v)}}{r}\right)+\mathbb{O}(h^6). \quad (43)$$

The nonstandard finite-difference approximation of $(1/r)(ru')'$ is

$$\frac{1}{rh}\left(\frac{u(r+h)-u(r)}{\log(r+h)-\log(r)}-\frac{u(r)-u(r-h)}{\log(r)-\log(r-h)}\right)=\frac{1}{r}(ru')'+\frac{h^2}{12}\left(u^{(iv)}+\frac{2u'''}{r}-\frac{u''}{r^2}+\frac{u'}{r^3}\right)$$
$$+\frac{h^4}{360}\left(u^{(vi)}+\frac{3u^{(v)}}{r}-\frac{5u^{(iv)}}{2r^2}+\frac{5u'''}{r^3}-\frac{19u''}{2r^4}+\frac{27u'}{2r^5}\right)+\mathbb{O}(h^6). \quad (44)$$

The standard finite-difference approximation of $(1/r^2)(r^2u')'$ looks like

$$\frac{1}{r^2h}\left(\left(r+\frac{h}{2}\right)^2\frac{u(r+h)-u(r)}{h}-\left(r-\frac{h}{2}\right)^2\frac{u(r)-u(r-h)}{h}\right)=\frac{1}{r^2}(r^2u')'$$
$$+\frac{h^2}{12}\left(u^{(iv)}+\frac{4u'''}{r}+\frac{3u''}{r^2}\right)+\frac{h^4}{360}\left(u^{(vi)}\frac{6u^{(v)}}{r}+\frac{15u^{(iv)}}{2r^2}\right)+\mathbb{O}(h^6). \quad (45)$$

The nonstandard finite-difference approximation of $(1/r^2)(r^2u')'$ is

$$\frac{1}{r^2h}\left(r\cdot(r+h)\frac{u(r+h)-u(r)}{h}-r\cdot(r-h)\cdot\frac{u(r)-u(r-h)}{h}\right)$$
$$=\frac{1}{r^2}(r^2u')'+\frac{h^2}{12}\left(u^{(iv)}+\frac{4u'''}{r}\right)+\frac{h^4}{360}\left(u^{(vi)}+\frac{6u^{(v)}}{r}\right)+\mathbb{O}(h^6). \quad (46)$$

The author thanks his thesis advisor Don Schwendeman of Rensselaer Polytechnic Institute for his useful suggestions and encouragement and Ronald Mickens of Clark Atlanta University for his friendliness and mentoring spirit. I also thank Tom Witelski of Duke University for apprising me of Professor Mickens's *oeuvre.* The numerical calculations for this article were performed using *Mathematica,* and the figures were generated using gnuplot. This article is dedicated to the memory of the late Julian D. Cole.

References

1. R. E. Mickens, Nonstandard finite difference schemes for differential equations, J Difference Eq Appl 8(9) (2002), 823–847.
2. R. E. Mickens, Applications of nonstandard finite differences, World Scientific, Singapore, 2000.
3. R. E. Mickens, Nonstandard difference models of differential equations, World Scientific, Singapore, 1994.
4. R. Buckmire, The design of shock-free transonic slender bodies of revolution. Ph.D. thesis, Rensselaer Polytechnic Institute, Troy, NY, 1994.
5. J. D. Cole and L. P. Cook, Transonic aerodynamics, North Holland, 1986.

6. J. D. Cole and N. Malmuth, Shock wave location on a slender transonic body of revolution. Mech Res Commun 16(6) (1989), 353–357.

7. J. D. Cole and A. F. Messiter, Expansion procedures and similarity laws for transonic flow. ZAMP 8 (1957), 1–25.

8. J. D. Cole and D. W. Schwendeman, Hodograph design of shock-free transonic slender bodies, Bjorn Engqvist and Bertil Gustafsson, editors, 3rd International Conference on Hyperbolic Problems, Uppsala, Sweden, June 11–15, 1990.

9. R. Buckmire, A new finite-difference scheme for singular boundary value problems in cylindrical or spherical coordinates, L. Pamela Cook and Victor Roytburd, editors, Mathematics is for solving problems, Society for Industrial and Applied Mathematics, Philadelphia, PA, 1996, pp 3–9.

10. R. E. Mickens and A. Smith, Finite-difference models of ordinary differential equations: Influence of denominator functions. J Franklin Instit 327 (1990), 143–145.

11. R. E. Mickens, Difference equation models of differential equations. Math Comput Model 11 (1988), 528–530.

12. J. A. Krupp and E. M. Murman, Computation of transonic flows past lifting airfoils and slender bodies, AIAA J 10(7) (1972), 880–886.

13. J. D. Cole and E. M. Murman, Calculation of plane steady transonic flows. AIAA J 9(1) (1971), 114–121.